



MARMARA UNIVERSITY
INSTITUTE FOR GRADUATE STUDIES
IN PURE AND APPLIED SCIENCES



**INVESTIGATION OF THE EFFECT OF TiO_2
FILM COATED ON HEMATITE PHOTOANODE
PRODUCED BY THERMAL OXIDATION ON
PHOTOELECTROCHEMICAL (PEC)
HYDROGEN PRODUCTION EFFICIENCY**

UĞUR OKTAY

MASTER THESIS

Department of Metallurgical and Materials Engineering

Thesis Supervisor

Prof. Dr. Cevat SARIOĞLU

ISTANBUL, 2024



MARMARA UNIVERSITY
INSTITUTE FOR GRADUATE STUDIES
IN PURE AND APPLIED SCIENCES



INVESTIGATION OF THE EFFECT OF TiO_2
FILM COATED ON HEMATITE PHOTOANODE
PRODUCED BY THERMAL OXIDATION ON
PHOTOELECTROCHEMICAL (PEC)
HYDROGEN PRODUCTION EFFICIENCY

UĞUR OKTAY

(524721005)

MASTER THESIS

Department of Metallurgical and Materials Engineering

Thesis Supervisor

Prof. Dr. Cevat SARIOĞLU

ISTANBUL, 2024

ACKNOWLEDGEMENTS

I would like to express my gratitude to my supervisor Prof. Dr. Cevat SARIOĞLU for his consistent support and guidance throughout my thesis. His experience and excitement in this research gave me the motivation to work.

I also would like to thank Associate Professor İsrail KÜÇÜK and Research Assistant Mehmet Emre AKÖZ from Gebze Technical University for providing the XPS measurements which was essential for my thesis.

I want to thank Research Assistant Şükrü KAYA, Research Assistant Alaaddin Cem OK, Research Assistant Fatma Betül YILMAZ GÜLER, Sercan SOYÖZ and Batuhan BAŞBOZKURT for their help and sharing their experiences.

And last but not least, I would like to thank my mother Zeynep OKTAY for her support, understanding and love during this period.

Uğur OKTAY

November, 2024

TABLE OF CONTENTS

| | |
|---|------|
| ACKNOWLEDGEMENTS..... | i |
| ABSTRACT..... | iv |
| ÖZET..... | v |
| SYMBOLS | vi |
| ABBREVIATIONS | vii |
| LIST OF FIGURES..... | viii |
| LIST OF TABLES | x |
| 1. INTRODUCTION..... | 1 |
| 1.1. The Hydrogen Energy | 2 |
| 1.2. Hydrogen Energy Production Methods | 2 |
| 1.3. Water Splitting via Solar Energy..... | 3 |
| 1.3.1. Photoelectrochemical water splitting | 4 |
| 1.4. Hematite Photoanodes | 4 |
| 1.4.1. Electrochemical deposition | 5 |
| 1.4.2. Thermal oxidation processes | 6 |
| 1.4.3. Surface modification techniques of hematite | 6 |
| 1.5. Photoelectrochemical Analysis | 7 |
| 1.5.1. Open circuit potential analyse | 7 |
| 1.5.2. Linear sweep voltammetry analyse | 8 |
| 1.5.3. Electrochemical impedance analyse..... | 9 |
| 1.6. UV-Vis Analyse | 9 |
| 1.7. X-ray Photoelectron Spectroscopy (XPS)..... | 10 |
| 1.8. Scanning Electron Microscopy (SEM) | 10 |
| 2. THE MATERIALS AND EXPERIMENTAL PROCEDURES | 11 |
| 2.1. Production Of The Bare And Modified Hematite Films | 11 |
| 2.1.1. Preparation of the electrolytic solution | 11 |
| 2.1.2. Preparation of the substrates..... | 12 |
| 2.1.3. Electrochemical deposition procedures..... | 12 |
| 2.1.4. Thermal oxidation steps | 12 |
| 2.1.5. Surface modification steps | 14 |
| 2.2. Evaluation And Characterizations | 16 |
| 2.2.1. Production of the photoelectrodes..... | 16 |

| | | |
|--------|---|-------------------------------------|
| 2.2.2. | Photocatalytic activity evaluation | 16 |
| 2.2.3. | UV-VIS analyse | 17 |
| 2.2.4. | X-ray photospectrometry (XPS) analyse | 17 |
| 2.2.5. | Scanning electron microscopy (SEM) analyse..... | 17 |
| 3. | RESULTS AND DISCUSSION | 18 |
| 3.1. | Effect of the Surface Modification | 18 |
| 3.1.1. | Photoelectrochemical tests | 18 |
| 3.1.2. | UV-Vis analysis | 26 |
| 3.1.3. | X-ray photospectrometry (XPS) analysis | 28 |
| 3.1.4. | SEM (Scanning electron microscopy) analysis..... | 29 |
| 4. | CONCLUSION | 30 |
| | REFERENCES | 31 |
| | CURRICULUM VITAE | Error! Bookmark not defined. |

ABSTRACT

INVESTIGATION OF THE EFFECT OF TiO₂ FILM COATED ON HEMATITE PHOTOANODE PRODUCED BY THERMAL OXIDATION ON PHOTOELECTROCHEMICAL (PEC) HYDROGEN PRODUCTION EFFICIENCY

The Hematite (α -Fe₂O₃) is a promising candidate for PEC water splitting due to its favorable band gap, abundance, and stability in aqueous environments. However, its efficiency is often limited by poor charge transport properties and rapid electron-hole recombination. To overcome these limitations, various methods can be used such as surface modification techniques in order to increase the PEC efficiency. The surface modification with using titanium dioxide has multiple benefits such as reducing electron-hole recombination, improving charge separation and optimizing some optical properties of the hematite. The aim in this study was to show the effect of titanium dioxide coating on the PEC characteristics of hematite (α -Fe₂O₃) photoanodes. Hematite samples were fabricated on FTO (Fluorine doped tin oxide) through electrochemical deposition of iron (Fe) followed with thermal oxidation process. Afterwards with the use of a water soluble titanium based solution including immersion followed with a heat treatment (calcination) a TiO₂ layer have been achieved on the surface of the hematite. It was observed that the PEC efficiency of hematite photoanodes have been moderately increased with this surface modification method. The PEC characterization of the samples have been made with LSV, OCP and EIS measurements and also XPS and UV-VIS spectrometry analysis conducted to analyse the titanium dioxide layer achieved on the surface of the hematite photoanode. The characterization of the surface morphology have been conducted with using the scanning electron microscopy (SEM).

ÖZET

TERMAL OKSİDASYONLA ÜRETİLEN HEMATİT FOTOANOT ÜZERİNE KAPLANAN TiO₂ FİLMİNİN FOTOELEKTROKİMYASAL (PEC) HİDROJEN ÜRETİM VERİMİNE ETKİSİNİN ARAŞTIRILMASI

Hematit (α -Fe₂O₃), elverişli bant aralığı, doğada yaygın olarak bulunması ve sulu ortamlardaki kararlılığı sebebiyle fotoelektrokimyasal su ayrıştırma yöntemi için umut vaat eden bir adaydır. Bununla birlikte, verimliliği genellikle zayıf yük taşıma özellikleri ve hızlı elektron boşluk rekombinasyonu ile sınırlıdır. Bu özellikleri iyileştirmek ve PEC verimliliğini artırmak amacıyla çeşitli yüzey modifikasyon teknikleri kullanılabilir. Titanyum dioksit kullanılarak yapılan yüzey modifikasyonunun elektron boşluk rekombinasyonunu azaltmak, yük ayrımını iyileştirmek ve hematitin bazı optik özelliklerini optimize etmek gibi olumlu etkileri bulunmaktadır. Bu çalışmanın amacı, titanyum dioksit kaplamanın hematit (α -FeO₃) fotoanotların PEC özellikleri üzerindeki etkisini göstermektir. Hematit numuneleri FTO (Flor katkılı kalay oksit) üzerine elektrokimyasal demir (Fe) biriktirme ve ardından termal oksidasyon işlemi ile üretilmiştir. Daha sonra suda çözünebilen titanyum bazlı bir çözelti kullanılarak hematit yüzeyinde bir TiO₂ tabakası elde edilmiştir. Bu yüzey modifikasyon yöntemi ile hematit fotoanotların PEC verimliliğinin orta derecede arttığı gözlemlenmiştir. Örneklerin PEC karakterizasyonu LSV, OCP ve EIS analizleri ile yapılmış ve ayrıca hematit fotoanot yüzeyinde elde edilen titanyum dioksit tabakasını analiz etmek için XPS ve UV-VIS spektrometri analizleri gerçekleştirilmiştir. Yüzey morfolojisinin karakterizasyonu taramalı elektron mikroskobu (SEM) kullanılarak gerçekleştirilmiştir.

SYMBOLS

| | |
|--|--------------------------------------|
| E | : Applied potential |
| J | : Current density |
| TiO₂ | : Titanium dioxide |
| α-Fe₂O₃ | : Iron oxide (α) hematite |
| pH | : Potential of hydrogen |
| Si | : Silicon |
| GaAs | : Gallium arsenide |
| n | : Direct/indirect allowed transition |
| GaP | : Gallium phosphide |
| Al₂O₃ | : Aluminium oxide |
| T | : Temperature |
| E_g | : Band gap energy |
| α | : Absorption coefficient |
| R_{ct} | : Charge transfer resistance |
| R_s | : Solution resistance |
| R_{sc} | : Space charge resistance |
| C_{sc} | : Space charge capacitance |
| C_h | : Helmholtz layer capacitance |

ABBREVIATIONS

| | |
|-------------|--|
| FTO | : Fluorine tin oxide |
| STH | : Solar to hydrogen |
| RE | : Reference electrode |
| SCE | : Saturated calomel electrode |
| TALH | : Titanium bis(ammonium lactate) dihydroxide |
| OCV | : Open circuit voltage |
| WE | : Working electrode |
| PEC | : Photoelectrochemical |
| OER | : Oxygen evolution half reaction |
| ALD | : Atomic layer deposition |
| HER | : Hydrogen evolution half reaction |
| CE | : Counter electrode |
| LSV | : Linear sweep voltammetry |
| RHE | : Reversible hydrogen electrode |
| XPS | : X-ray photoelectron spectroscopy |
| SEM | : Scanning electron microscopy |
| EIS | : Electrochemical impedance spectroscopy |

LIST OF FIGURES

| | |
|--|----|
| Figure 1. 1. Schematic representation of a photoelectrochemical (PEC) water-splitting system [1]. | 4 |
| Figure 1. 2. The illustration of electrochemical deposition of iron (Fe) on FTO [2]. | 5 |
| Figure 1. 3. The photopotential response of the hematite (α -Fe ₂ O ₃) photoanode produced in air atmosphere under the illuminated and dark conditions. | 8 |
| Figure 2. 1. Thin Fe coating with using electrodeposition in a electrode system with two-electrodes on the FTO substrate | 12 |
| Figure 2. 2. Fe coated samples before the oxidation procedure. | 13 |
| Figure 2. 3. The hematite achieved samples after the oxidation procedure. | 13 |
| Figure 2. 4. The setup for the oxidation in argon atmosphere, a furnace with a tube have been utilized. | 13 |
| Figure 2. 5. Furnace setup for the thermal oxidation in air atmosphere. | 14 |
| Figure 2. 6. Prepared hematite (α -Fe ₂ O ₃) samples on the immersion step inside 2.5 mmol/TALH solution. | 14 |
| Figure 2. 7. The hematite photoanode prepared with using a conductive silver paste and a conductive copper wire. | 16 |
| Figure 2. 8. Photoelectrochemical measurement setup with the 3 electrode system, using a solar simulator for the illumination. | 17 |
| Figure 3. 1. Open circuit potential analysis of bare hematite produced in the air atmosphere at 550 °C for 30 minutes. | 19 |
| Figure 3. 2. Open circuit potential analysis of surface modified hematite, immersed in 0.5 mmol/L TALH solution for 1 hour and calcinated in air atmosphere at 350 °C for 1 hour. | 19 |
| Figure 3. 3. Open circuit potential analysis of surface modified hematite, immersed in 5.0 mmol/L TALH solution for 1 hour and calcinated in air atmosphere at 350 °C for 1 hour. | 20 |
| Figure 3. 4. Open circuit potential analysis of surface modified hematite, immersed in 2.5 mmol/L TALH solution for 1 hour and calcinated in air atmosphere at 350 °C for 1 hour. | 20 |
| Figure 3. 5. LSV analysis under dark and illuminated conditions. Bare hematite produced in air atmosphere, surface modified hematite samples were immersed in TALH solutions for 1 hour and calcinated in air atmosphere at 350°C for 1 hour. | 21 |
| Figure 3. 6. LSV analysis of modified hematite samples. Immersed in 0.5 mmol/L TALH solution with various immersion times (40-60 min), afterwards calcinated in argon atmosphere at 350°C for 1 hour. | 22 |
| Figure 3. 7. LSV analysis of modified hematite samples. Immersed in 2.5 mmol/L TALH solution with various immersion times (20-30 min), afterwards calcinated in argon atmosphere at 350°C for 1 hour. | 22 |
| Figure 3. 8. LSV analysis of modified hematite samples. Immersed in 5.0 mmol/L TALH solution with various immersion times (5-10 min), afterwards calcinated in argon atmosphere at 350°C for 1 hour. | 23 |

| | |
|--|----|
| Figure 3. 9. LSV analysis of surface modified samples with various calcination temperatures. Immersed in 2.5 mmol/L TALH solution for 1 hour, calcinated at various temperatures (350-450-550 °C) in argon atmosphere for 1 hour. | 23 |
| Figure 3. 10. Equivalent circuit model illustration that used in the impedance analysis. | 24 |
| Figure 3. 11. Nyquist plots (z-fitted) of the bare and titanium modified hematite samples under illuminated conditions. Bare hematite produced in argon atmosphere, Ti-modified hematite sample immersed in 2.5 mmol/L TALH solution for 1 hour and calcinated in argon atmosphere at 350 °C for 1 hour. | 25 |
| Figure 3. 12. Shows the UV-Vis absorption spectra of the samples. Bare hematite produced in air and argon atmosphere, titanium modified hematite immersed in 2.5 mmol/L TALH solution for 1 hour and calcinated in argon atmosphere at 350 °C for 1 hour. | 26 |
| Figure 3. 13. Shows the Tauc Plots of bare and titanium modified hematite samples..... | 27 |
| Figure 3. 14. XPS analysis of the bare and titanium modified hematite samples focused in the binding energy range of 450-474 eV. Ti-modified hematite sample immersed in 2.5 mmol/L TALH solution for 1 hour and calcinated in argon atmosphere at 350 °C for 1 hour..... | 28 |
| Figure 3. 15. SEM micrographs of the a) bare hematite produced in argon atmosphere b) titanium modified hematite, immersed in 2.5 mmol/L TALH for 1 hour, calcinated in argon atmosphere at 350 °C for 1 hour. | 29 |

LIST OF TABLES

| | |
|---|----|
| Table 2. 1. The details of the thermal oxidation process. | 13 |
| Table 2. 2. The details of the TALH immersion processes of hematite samples produced in air atmosphere. | 15 |
| Table 2. 3. The details of the TALH immersion processes of hematite samples produced in argon atmosphere. | 15 |
| Table 2. 4. Details of the calcination processes of hematite samples produced in argon atmosphere. | 15 |
| Table 2. 5. Details of the calcination processes of hematite samples produced in air atmosphere. | 16 |
| Table 3. 1. Fitting results for EIS analysis of the samples. | 25 |



1. INTRODUCTION

The global need for energy relies greatly on fossil fuels, resulting in high levels of carbon emissions in the air. As a result, clean energy sources are essential to preserve the environment due to increasing energy requirements. Hydrogen energy is gaining significant attention as a renewable energy source due to its abundance, environmental friendliness, and its potential to reduce carbon dioxide emissions. Ongoing researches are focused on identifying cost-effective and efficient methods for hydrogen energy production. Among these methods, photoelectrochemical (PEC) water splitting stands out as a promising technique, as it generates hydrogen gas by utilizing solar energy by splitting water [1].

In photoelectrochemical hydrogen production, water is split into hydrogen and oxygen gases. At an n-type photoanode, oxygen gas is produced when an anodic voltage is applied, while hydrogen gas forms at the cathode. Conversely, in systems using p-type semiconductor materials, the photocathode operates under a cathodic voltage, resulting in hydrogen gas generation at the photocathode and oxygen gas evolution at the anode. [1-2].

Hematite ($\alpha\text{-Fe}_2\text{O}_3$) has garnered significant interest as a photoelectrode (photoanode) due to its low cost, abundance in nature, ability to absorb a broad spectrum of sunlight, optimized and ideal bandgap of 2.0 eV, and stability as an iron oxide in aqueous environments [1]. As claimed by the previous studies that have been investigated in this field, there are some boundaries have been discovered that limiting the PEC efficiency of the hematite [2]. The subpar properties of hematite electrodes has been linked to their inadequate current-carrying capacity, limited hole diffusion distance, and the need for high overvoltage. In order to improve the PEC efficiency of hematite there are several approaches are being used such as doping, surface passivation, nanostructuring, Co-catalyst loading and heterojunction formation [1-2].

In the literature, it has been reported that the surface modification of hematite with using a titanium based solution has dramatically improved the photocurrent density of the hematite [3]. Studies have shown that applying a TiO_2 coating on hematite creates a passivation layer that reduces surface recombination while enhancing charge separation and transport properties in the hematite photoanode. [2-3]. Additionally, the TiO_2 coating has been enhanced the catalytic activity and optimize light absorption. These combined effects significantly improve the

photoelectrochemical (PEC) performance of hematite photoanodes, boosting their efficiency for solar water splitting and other PEC applications. [2].

This study has been focused on the producing an overlayer on hematite with the use of a titanium based solution, and afterwards investigated the effects in the terms of PEC efficiency. The hematite ($\alpha\text{-Fe}_2\text{O}_3$) films were produced with heat treatment of Fe films that were electrodeposited onto FTO substrates at 550°C in different gas environments (air, argon), afterwards with using a basic surface modification technique the TiO_2 coating have been achieved on the surface of the as prepared hematite ($\alpha\text{-Fe}_2\text{O}_3$) and the prepared electrodes have been evaluated with the PEC characterizations such as OCP, LSV and EIS measurements respectively and for the characterization of TiO_2 coating XPS, UV-VIS and SEM analysis have been conducted.

1.1. The Hydrogen Energy

Hydrogen is the superabundant component in nature, however, it rarely exists on its own in nature. Instead, it is considered as a auxiliary energy, it is generated from fundamental, common energy sources like carbon based fuels. Hydrogen production can come from both carbon based fuels and sustainable sources, but it needs to be generated from eco-friendly energy sources to be considered an environmentally friendly energy carrier [2-4]. Studies suggest that the energy requirements of the population could be met by less than 1% of solar energy [1]. Hydrogen has the potential to serve as a source of power for electricity generation and offers a promising pathway toward a carbon-neutral energy resource.

According to the recent scientific advancements, it might soon be possible to generate cheaper electricity and hydrogen by using semiconductor materials [1]. One of the most promising approaches in that concept is PEC water splitting which uses photoelectrochemical methods for the direct conversion of water to hydrogen. However, still the use of a large-scale utilization of this method remains one of the most significant challenges in this application [21].

1.2. Hydrogen Energy Production Methods

Fossil fuels are such as coal and oil and the eco-friendly energy sources like solar, wind, and hydropower are sources of hydrogen energy. Various industries has been using the hydrogen energy for rocket fuel and chemical reactions for over fifty years. Hydrogen was produced at the time by burning fossil fuels, but as the population grew and technology advanced, so did

the utilization of fossil fuels. In the outcome the less fossil fuel reserves and more greenhouse gas emissions achieved. Therefore, in order to the hydrogen energy to remain environmentally friendly and sustainable, it must be produced using renewable and sustainable power sources. Biochemical or thermochemical processes that use biomass as a feedstock can produce hydrogen. Additionally, it can be produced by water splitting, thermolysis, and photolysis. Solar-powered water splitting generates hydrogen without emitting greenhouse gases. This process reduces reliance on fossil fuels and meets energy demands with minimal environmental impact. These advantages positions the PEC water splitting as one of the most promising methods for hydrogen production in the future. [4].

1.3. Water Splitting via Solar Energy

The energy of the photon is converted into the chemical energy through water splitting, leading to a primarily favorable shift in the Gibbs free energy. Because of the reaction that occurs which is similar to photosynthesis, water splitting through photocatalysis is recognized as the artificial photosynthesis. In photocatalytic and photoelectrochemical water splitting there are two techniques that use photon energy to split water. Compared to electrochemical photosynthesis water splitting, through photocatalysis is more basic and also less expensive application. Furthermore, producing hydrogen on a large scale sustainably can be achieved through photocatalytic water splitting. Nevertheless, the primary drawback of this approach is the requirement to isolate evolved hydrogen from oxygen. In contrast, hydrogen can be extracted independently from oxygen using photoelectrochemical water splitting. For post-separation, a strong energy penalty is not required [5]. Even if a material does not have the potential to split water focused on the electronic band structure, it might be possible to do so with the utilization of an external bias. It can also be performed at ambient temperatures without requiring large-scale sun-focused mirrors. Using inorganic materials instead of organic or biological ones provides photoelectrochemical water-splitting devices with enhanced chemical stability and durability, offering an additional advantage. [2,4-5,6].

In this study, the surface of the hematite has been modified with titanium dioxide and used as a photoanode for the generation of hydrogen by solar energy with using the water splitting through photoelectrochemical method.

1.3.1. Photoelectrochemical water splitting

Photoelectrochemical (PEC) water splitting converts water (H_2O) into hydrogen (H_2) and oxygen (O_2) through a chemical reaction powered by solar energy. This method is regarded as one of the most promising approaches to producing sustainable hydrogen fuel because it converts solar energy directly into chemical energy in the form of hydrogen, which can be stored and used as a clean energy source. The water-splitting via photoelectrochemical processes involves sunlight absorption through the use of a semiconductor material that generates electron-hole couples in order to execute the redox process, which are the oxidation and reduction of water to produce oxygen gas and hydrogen gas.

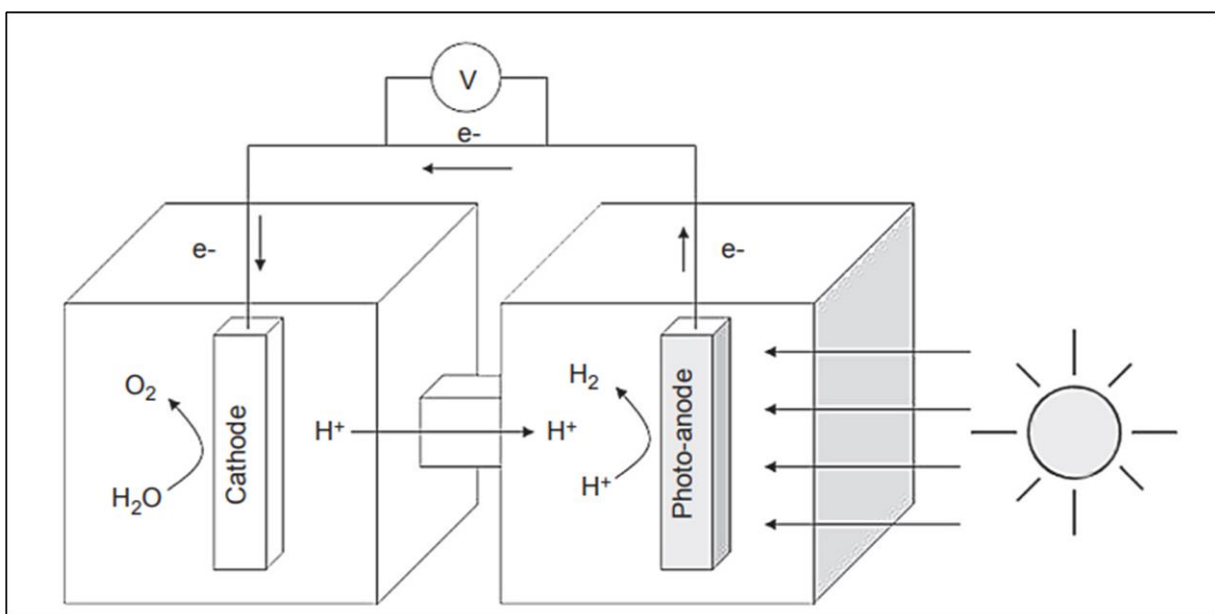


Figure 1. 1. Schematic representation of a photoelectrochemical (PEC) water-splitting system [1].

An efficient photoelectrode to be used in this processes, must have the following essential components: (1) appropriate VB (valance band) and CB (conduction band) energies for H_2 and O_2 generation reactions (2) effective separation and fine charge transport; (3) produced into photoelectrodes at a reasonable cost; (4) great stability in an water environment; (5) efficient absorption of visible light. Figure 1.1. presents the principle of a basic PEC water splitting system [1].

1.4. Hematite Photoanodes

The metal oxides spesifically hematite, due to their natural property, it is readily synthesized and can be found in large quantities in nature. For solar hydrogen production, the hematite (α -

Fe_2O_3) is one of the typically used oxide semiconductor. Using hematite as a photoanode, photoelectrochemical driven water splitting offers a great deal of potential for utilizing solar energy to produce hydrogen. Hematite has many beneficial characteristics, including being widely available in nature, being environmentally friendly, having a considerably constricted band gap (1.9–2.2 eV), being highly photochemically stable, and having the potential to reach a theoretical ultimate solar-to-hydrogen capability of 15.4%. Nonetheless, this material suffers from poor electrical conductivity, short excited-state lifetime (10~6 s), slow oxygen evolution reaction kinetics, short hole diffusion length (2–4 nm), and limited light absorption capacity which creates a number of routes for electron–hole recombination in the bulk and at interfaces and surfaces. These limitations severely effects the hematite photoanodes PEC activity. Various approaches have been investigated to enhance the properties of the hematite, surface modifacation with using passivation, cocatalyst and back reactions are the comman methods that have been used in the literature [2-5-6-7].

1.4.1. Electrochemical deposition

The electrochemical deposition is a straightforward, economical, and environmentally benign technique for creating Fe thin films at room temperature with the use of an electrolyte. Electrochemical deposition may occur in three various methods: cathodic, anodic, or both of them. Applying a negative potential to an electrolyte solution containing iron ions, a two-electrode system can be used to perform electrodeposition with using the cathodic technique. [7-8].

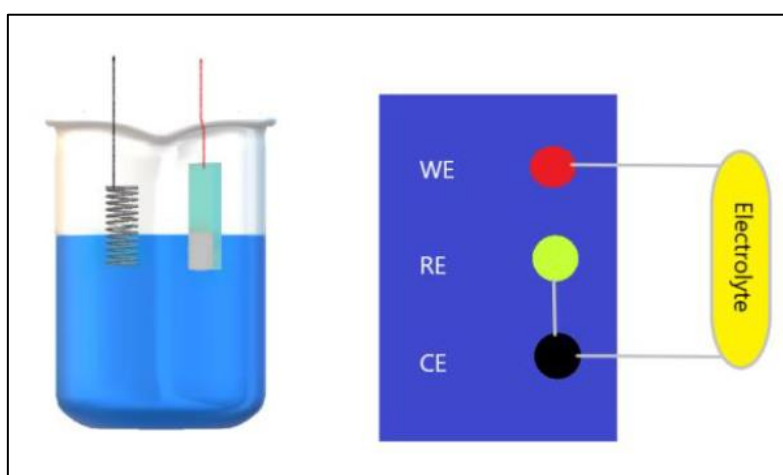


Figure 1. 2. The illustration of electrochemical deposition of iron (Fe) on FTO [2]

In this experimental study, the deposition of Fe film has been performed with a dual-electrode electrochemical setup with using a iron (Fe^{+2}) ions containing solution. Figure 1.2. illustrates

this electrochemical deposition setup which is containing a counter electrode and a working electrode [2].

1.4.2. Thermal oxidation processes

The thermal oxidation is an economical, single-step process which doesn't require expensive or specialized equipment. In the literature it has been described that the development of the hematite thin films are mainly effected with the oxidation temperature, time and the atmosphere of the heat treatment (thermal oxidation) process. Rapid heating, heating rate and cooling rates are also the parameters that effects the PEC properties of the hematite. It has been observed that increasing the oxidation time and temperature in a low-oxygen environment improves the photocurrent density of hematite photoanodes. With the different controlled oxidation environments, various heating temperatures and time, the hematite morphology changes, and it effects the photoelectrochemical performance of the hematite photoanode [2-16]. Therefore in this study the thermal oxidation process step for the generation of the hematite film, has been performed in argon and air atmospheres respectively in order to present the effect of the oxidation atmospheres.

1.4.3. Surface modification techniques of hematite

The surface modification of hematite can be achieved with various methods and techniques such as doping, the passivation of the surface, catalyst deposition, core-shell structures and nanostructuring [7]. The heterojunction structure of hematite ($\alpha\text{-Fe}_2\text{O}_3$) and another semiconductor can create an internal electric field at contact regions, resulting as an effective carrier separation and increased PEC activity. Using the passivation overlayers on semiconductor photoelectrode surfaces have recently gained significant attention as an effective strategy to improve charge transfer and separation at semiconductor-liquid interfaces. [9]. For instance, applying a thin TiO_2 coating to the surface of Si, GaAs, and GaP photoanodes via atomic layer deposition (ALD) has been shown to profoundly improve their stability and water oxidation efficiency [9-10]. In contrast to this, in another study, TiO_2 overlayers showed no beneficial effect, according to Le Formal et al., but an Al_2O_3 overlayer deposited by atomic layer deposition (ALD) can reduce the overpotential required for the water oxidation on the hematite photoanodes by up to 100 mV [19]. In a reexamination of the effects of a 100 mV reduction in the overpotential required for water oxidation on hematite photoanodes, Yang et al. found no benefit from TiO_2 overlayers. Yang and associates reexamined the effects of

ultrathin TiO₂ deposits made with the ALD method on hematite photoanode performance. Despite achieving a cathodic transition of approximately 100 mV, there was no noticeable enhancement of the response of the photocurrents [11]. A substitute for the ALD method, some titanium based solutions can be used to achieve a TiO₂ coating on the hematite surface. Using precursors that contain TiCl₄ immersion of the hematite and followed with a heat treatment TiO₂ overlayers can also be achieved [13]. Alternatively in another work in the literature, with using a titanium based water soluble solution (i.e., titanium bis(ammonium lactate) dihydroxide, TALH) the TiO₂ overlayer on hematite can also be achieved. TALH solution complex is a precursor that has negatively charged, and depending on the pH of the solution, the hematite which is in the surface hydroxyl group can become either protonated (positively charged) or deprotonated (negatively charged) [3-14]. Hematite's point of zero charge (PZC) is known to be between pH 7 and pH 9.5 [3-20]. Therefore, at a pH level lower than the hematites PZC, its surface can be electropositively charged. In these conditions the submersion of the hematite in a titanium containing solution will lead to the Ti⁺ ions to migrate on the surface of the hematite. Afterwards the immersion step a gentle heat treatment (calcination) to this sample lead to the formation of a TiO₂ overlayer on the surface of the hematite.[3-15]. In this experimental study this principle have been used in order to achieve the TiO₂ coating on the surface of the hematite samples which were produced with thermal oxidation of Fe thin films.

1.5. Photoelectrochemical Analysis

The photoelectrochemical analysis are conducted to provide an insight to the behavior of an electrolyte or semiconductor and photoelectrodes that are effective at water splitting process under illuminated conditions. In this experimental study it has been used LSV (linear sweep voltammetry), OCV (open circuit voltage) and EIS (impedance spectroscopy) to analyse the photoelectrochemical behaviors of the samples. The analysis performed with the photoanode sample, platinum wire, and SCE (saturated calomel electrode) a three-electrode technique that comprises a CE (counter electrode), WE (working electrode), and a RE (reference electrode) [2].

1.5.1. Open circuit potential analyse

The open circuit potential measurement shows the equilibrium potential of a semiconductor/electrolyte interface under no external bias. The amount of the voltage difference, between the semiconductor used as the WE and the RE in a dark environment

compared to the illuminated environment have been measured by open circuit voltage. OCV can provide details regarding a semiconductor's resistance to corrosion [17]. This analysis can also be used to determine the conductivity type because semiconductor materials are photosensitive. The photovoltage response is recorded and plotted over time in both illuminated and dark circumstances. If the potential goes to the positive side under illuminated conditions, this refers that the semiconductor material is p-type; if the potential shifts towards the negative side it shows that the material is n-type [2]. Here in Figure 1.3. we see the potential decreases when the light is on, which shows that this photoanode sample is photosensitive n-type photoanode.

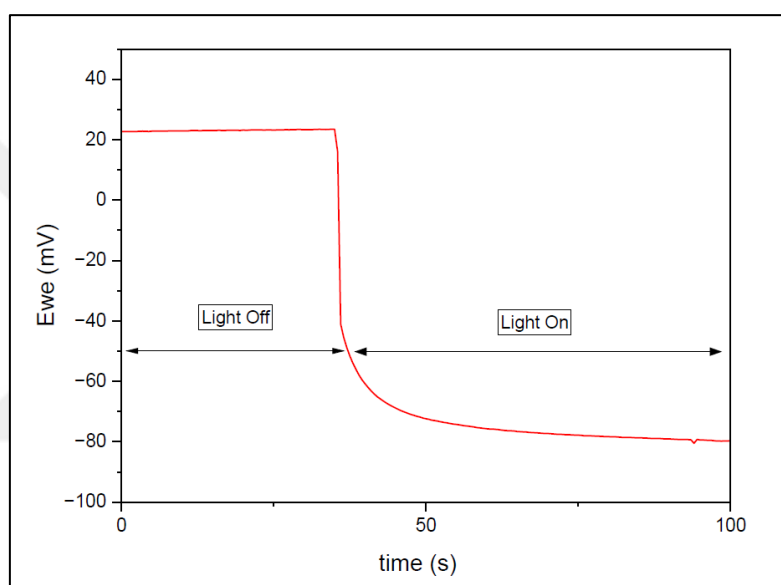


Figure 1. 3. The photopotential response of the hematite (α - Fe_2O_3) photoanode produced in air atmosphere under the illuminated and dark conditions.

1.5.2. Linear sweep voltammetry analyse

The linear sweep voltammetry or referred as J-V curves represent the relationship between the current density (J) and the applied voltage (V) in a photoelectrochemical cell. The primary applications of this measurement technique are in the assessment of the current density at the reversible potential for the oxygen evolution reaction (OER) and the hydrogen evolution reaction (HER). Two methods are being used to measure the light-driven current response: in the shaded and in the light irradiated environment. The J-V plot shows that the majority of charge carriers move from the valence to the conduction band when the semiconductor is exposed to light that has an energy that is equal to or greater than its bandgap energy. It is important to know the type of conductivity of the sample before this experiment, because when

a n-type based semiconductor material is used, the photogenerated current is determined at the anodic region area under light irradiation. In contrast, the photocurrent needs to be determined in the negative potential area when dealing with p-type semiconductor materials [18].

$$E_{RHE} = E^{\circ}_{Hg/Hg_2Cl_2} + E_{Hg/Hg_2Cl_2} + 0,059 * pH \quad (1.1)$$

$$E_{RHE} = 0,241 + E_{Hg/Hg_2Cl_2} + 0,7$$

$$E_{RHE} = 1,01 + E_{Hg/Hg_2Cl_2}$$

With using the equation (1.1) we can convert the monitored potential results versus SCE (saturated calomel electrode) to the related results versus RHE (the reversible hydrogen electrode) [18].

1.5.3. Electrochemical impedance analyse

With the causing reactions at the counter electrode when an AC potential is given to an electrochemical cell, impedance determines the current passing through the cell. Impedance measurements using a potentiostat can provide insight into the sample's electrochemical behaviors. With using this measurement, we achieve the nyquist graphs, with this data we can determine the hematite-electrolyte interface behaviors, as well as the bulk material's resistance and capacitance, by measuring impedance [1-2].

1.6. UV-Vis Analyse

The UV-Vis analyse basically measures the absorbance (or transmittance) of the light in the ultraviolet (UV) and visible (Vis) regions of the light spectrum which consists the lights in the wavelength range of 200-800 nm. When the light passes through or reflected by the material the certain wavelngts are absorbed due to the electronic transitions in the material. This phenomena produces an absorbance spectrum characteristic of the material's properties. In the semiconductor materials it provides information about the optical band-gap according to the electrical transitions taking place between the valance and the conduction bands of the samples [2-18]. The indirect and direct optical band gaps can be evaluated by The Tauc plot produced from the Tauc model in Equation (1.2), it shows the correlation between the absorption coefficient (α), photon energy ($h\nu$), and the band gap of the materials [2-18].

$$\alpha h\nu = A (h\nu - E_g)^n \quad (1.2)$$

1.7. X-ray Photoelectron Spectroscopy (XPS)

The XPS is a sensitive surface analysis technique which is used for the investigation of the elemental composition, electronic structures and chemical states of the materials. The working mechanism of XPS consists of the use of X-rays (commonly Al K α , 1486.6 eV) in order to irradiate the surface of the material. With this irradiation it ejects the core electrons from atoms which are present in the material [23-24].

The kinetic energy (KE) of the ejected electrons from the core is measured with the use of the photoelectric equation (1.3) [23-24].

$$BE = h\nu - KE - \phi \quad (1.3)$$

BE = Binding Energy

$h\nu$ = Photon energy

ϕ = Work function

Since the binding energy is particular for each element and its chemical environment, we can learn information about the elemental and chemical states and use this data for the identification of the materials [23-24].

1.8. Scanning Electron Microscopy (SEM)

Scanning Electron Microscopy (SEM) is a powerful imaging technique for analyzing the surface morphology and topographical features of materials at a high resolution. In SEM, a focused beam of electrons is directed at the sample. These electrons interact with the atoms of the material, producing various signals such as secondary electrons, backscattered electrons, and X-rays. These signals are then collected to generate highly detailed images and provide information about the sample's composition, texture, and structure.

The SEM uses various detectors and modes to obtain different types of information. The secondary electron detectors are used to capture secondary electrons emitted from the sample surface when it is bombarded by the electron beam, it gives high-resolution images of the surface morphology and revealing fine surface features and textures. This mode is typically applied in high vacuum conditions to provide clear surface images [25].

2. THE MATERIALS AND EXPERIMENTAL PROCEDURES

In this section the selected materials, methods and the selected experimental procedures are explained that used in this study. Since this study has been focused on the PEC effects of the TiO₂ coating, the comparison between bare and titanium modified hematite samples were discussed. According to the previous studies the most efficient parameters were taken as referances here and used in the fabrication of the hematite to achieve the highest photo electrochemical potential [2].

2.1. Production Of The Bare And Modified Hematite Films

The fabrication of the hematite thin films in this experiment consists of two stages. In the first stage the iron (Fe) was electrodeposited onto the FTO substrate with use of an iron containing electrolyte solution. The second stage involves the oxidation of thin iron film, with this process iron films are transformed into the hematite (α -Fe₂O₃).

2.1.1. Preparation of the electrolytic solution

In this investigation, the Fe film preparation was carried out with a hydrated Iron (II) sulfate concentrations in electrolytic bath solution. 50 milliliters of distilled water, 0.02 M of Iron(II) sulfate (FeSO₄.7H₂O), 0.5 M hydroxyboric acid (H₃BO₃), 0.5 M sodium sulfate (Na₂SO₄), and 0.5 M hydroxyboric acid (H₃BO₃) make up the electrolytic solution for the electrodeposition [2]. The Iron(II) sulfate acts as the primary iron source in this solution. During the electrodeposition process iron ions (Fe⁺²) deposited on the substrate of the FTO. Boric acid here used acts as the buffering agent in this solution, helps maintaining the pH of the solution which is crucial for the controlling of the deposition rate and the quality of the iron film and it also helps to create a smooth surface. Sodium sulphate provides ionic conductivity to the solution and ensuring that there is a steady flow of ions within the electrolyte during the electrodeposition process. This helps in maintaining a consistent electric field across the electrodes whic is important for the uniform deposition. The distilled water acts here as a solvent for the other components, ensuring that they are disolved uniformly and the solution is free from impurities that could interfere with the electrodeposition process.

2.1.2. Preparation of the substrates

In order to deposit a homogenous Fe layering on the substrate, the fluorine-doped tin oxide (FTO) samples were properly cleaned with using ultrasonic rinsing in acetone, ethyl alcohol, and deionized water for each 20 minutes and then promptly dried with a rubber air blower immediately afterwards.

2.1.3. Electrochemical deposition procedures

In the electrochemical deposition process a galvanostat used in Figure 2.1. A binary electrode setup cell operating in a electrostatic mode was used to prepare Fe thin layers on FTO through electrodeposition. The working electrode, which is an FTO substrate, and the counter electrode, which is a platinum wire, were separated by approximately 1.5 cm during the deposition process. The current densities were kept as $5 \text{ mA} / \text{cm}^2$, and the deposition time was 50 s for all samples.



Figure 2. 1. Thin Fe coating with using electrodeposition in a electrode system with two-electrodes on the FTO substrate

2.1.4. Thermal oxidation steps

In a Protherm tube furnace the thermal oxidation of Fe thin films have been conducted to accomplish a homogenous hematite on the surface of the FTO. Here in the oxidation process the parameters were kept at 550°C for 24 hours in argon atmosphere and 550°C for 30 minutes in air atmosphere. According to the previous studies these parameters were selected in order to achieve the highest PEC efficiency of the hematite photoanodes [2]. The oxidation process conducted under the flow of argon gas containing environment, the rate of argon gas was set to (1.5 L/min) for half an hour just before starting the test. After starting the test, the argon gas

flush was stabilized to 0.3 L/min until the end of the test. For all thermal oxidation and calcination steps the heat rate of the samples were kept as 10°C/min.

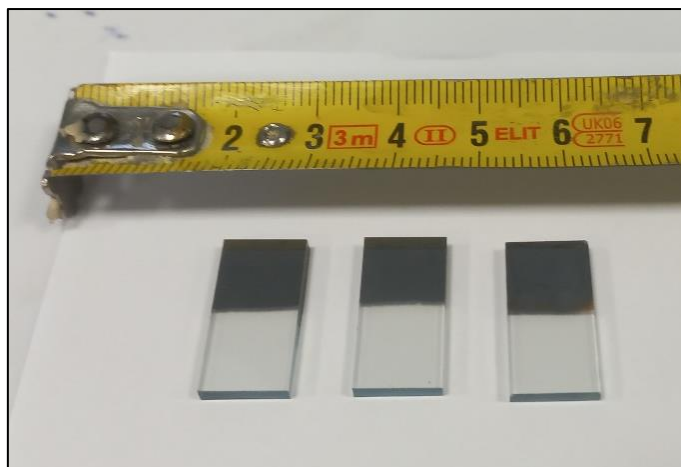


Figure 2. 2. Fe coated samples before the oxidation procedure.

Table 2. 1. The details of the thermal oxidation process.

| Sample | Atmosphere | Oxidation Temperature | Time |
|---------------------|------------|-----------------------|--------|
| Bare Hematite-Air | Air | 550 °C | 30 min |
| Bare Hematite-Argon | Argon | 550 °C | 24 h |



Figure 2. 3. The hematite achieved samples after the oxidation procedure.

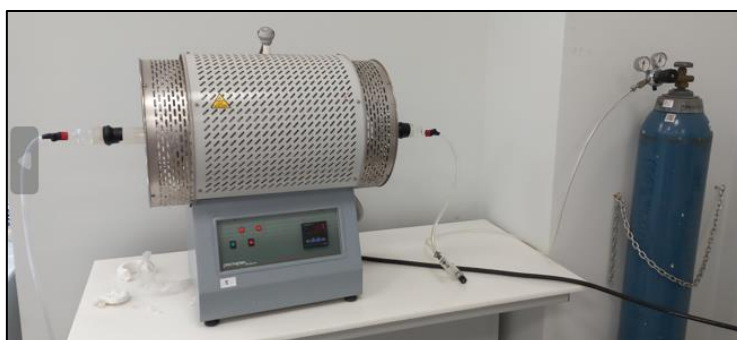


Figure 2. 4. The setup for the oxidation in argon atmosphere, a furnace with a tube have been utilized.



Figure 2. 5. Furnace setup for the thermal oxidation in air atmosphere.

2.1.5. Surface modification steps

For the surface modification, various concentrations of TALH solutions (0.5, 2.5, and 5 mmol L⁻¹) have been prepared. The prepared hematite samples were carefully immersed in the solutions for various immersion times. Afterwards they cleaned with pure water and dried immediately. For the next step in order to achieve the titanium dioxide layer on the hematite, the samples were heat treated (calcinated) at various temperatures for 1 hour. For all thermal oxidation and calcination steps, samples heating rate was 10°C/min. Following the test, the samples were left to cooldown to room temperature at the oven.

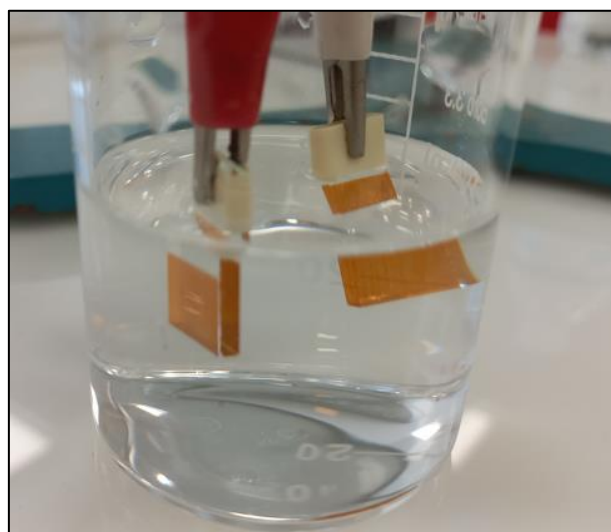


Figure 2. 6. Prepared hematite (α -Fe₂O₃) samples on the immersion step inside 2.5 mmol/ TALH solution.

Table 2. 2. The details of the TALH immersion processes of hematite samples produced in air atmosphere.

| Sample | Solution pH | TALH Concentration | Immersion Time |
|----------|-------------|--------------------|----------------|
| 0.5-TALH | 4.5 | 0.5 mmol/L | 60 min |
| 2.5-TALH | 4.5 | 2.5 mmol/L | 60 min |
| 5.0-TALH | 4.5 | 5.0 mmol/L | 60 min |

Table 2. 3. The details of the TALH immersion processes of hematite samples produced in argon atmosphere.

| Sample | Solution pH | TALH Concentration | Immersion Time |
|------------|-------------|--------------------|----------------|
| 0.5-TALH-1 | 4.5 | 0.5 mmol/L | 40 min |
| 0.5-TALH-2 | 4.5 | 0.5 mmol/L | 60 min |
| 2.5-TALH-1 | 4.6 | 2.5 mmol/L | 20 min |
| 2.5-TALH-2 | 4.6 | 2.5 mmol/L | 30 min |
| 5.0-TALH-1 | 4.7 | 5 mmol/L | 5 min |
| 5.0-TALH-2 | 4.7 | 5 mmol/L | 10 min |
| 350 HT | 4.6 | 2.5 mmol/L | 60 min |
| 450 HT | 4.6 | 2.5 mmol/L | 60 min |
| 550 HT | 4.6 | 2.5 mmol/L | 60 min |

Table 2. 4. Details of the calcination processes of hematite samples produced in argon atmosphere.

| Sample | Calcination Atmosphere | Calcination Temperature | Calcination Time |
|------------|------------------------|-------------------------|------------------|
| 0.5-TALH-1 | Argon | 350 °C | 1 h |
| 0.5-TALH-2 | Argon | 350 °C | 1 h |
| 2.5-TALH-1 | Argon | 350 °C | 1 h |
| 2.5-TALH-2 | Argon | 350 °C | 1 h |
| 5.0-TALH-1 | Argon | 350 °C | 1 h |
| 5.0-TALH-2 | Argon | 350 °C | 1 h |
| 350 HT | Argon | 350 °C | 1 h |
| 450 HT | Argon | 450 °C | 1 h |
| 550 HT | Argon | 550 °C | 1 h |

Table 2. 5. Details of the calcination processes of hematite samples produced in air atmosphere.

| Sample | Calcination Atmosphere | Calcination Temperature | Calcination Time |
|----------|------------------------|-------------------------|------------------|
| 0.5-TALH | Air | 350 °C | 1 h |
| 2.5-TALH | Air | 350 °C | 1 h |
| 5.0-TALH | Air | 350 °C | 1 h |

2.2. Evaluation And Characterizations

2.2.1. Production of the photoelectrodes

In order to carry out the photoelectrochemical measurements of the semiconductor, a copper wire has been used. To accomplish an efficient electrical conductivity, silver paste have been used to make the contact between the FTO surface and the copper wire. Afterwards the contact areas were covered carefully with a hot glue gun. The working electrodes surface area has been arranged to be approximately 1 cm² for all samples.

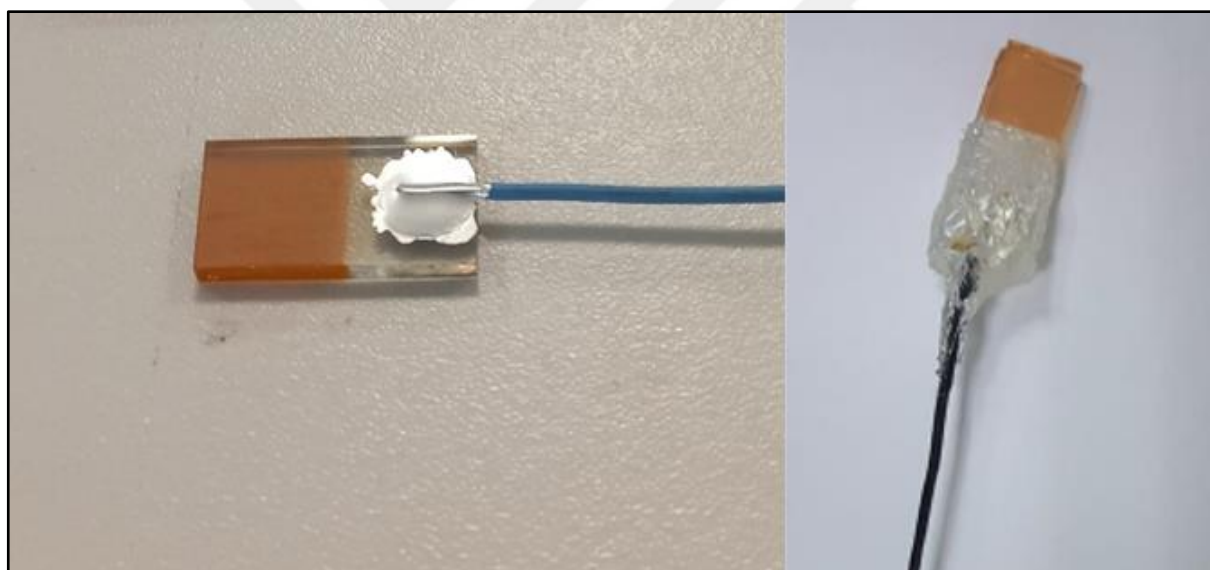


Figure 2. 7. The hematite photoanode prepared with using a conductive silver paste and a conductive copper wire.

2.2.2. Photocatalytic activity evaluation

All samples were connected to copper wire with using a conductive silver paste and a hot glue to form the photoelectrodes. Photoelectrochemical measurements, including OCP, LSV and EIS analysis, were performed in a three-electrode setup. The reference electrode used was a saturated calomel electrode (SCE), the counter electrode used was a platinum wire, and the hematite photoanode served as the working electrode. These experiments were conducted in a

0.1 M sodium hydroxide electrolyte, with the utilization of a potentiostat (Bio-Logic VSP). The measurements were carried out under AM 1.5G solar irradiation provided by an Abet solar simulator, with the hematite photoanode being exposed to a light intensity of 1000 W/cm². In order to arrange the light intensity the distance between the tip of the solar simulator and the photoanode for all samples arranged as 3 cm approximately during the analysis.



Figure 2. 8. Photoelectrochemical measurement setup with the 3 electrode system, using a solar simulator for the illumination.

2.2.3. UV-VIS analyse

The band gap of the samples were measured with using a UV-VIS-NIR spectrometer (Shimadzu 3600) over a wavelength range of 400 nm to 800 nm. Afterwards with using the equation 1.2. the bandgaps of the samples are calculated.

2.2.4. X-ray photospectrometry (XPS) analyse

The XPS analysis conducted with SPECS XRC 1000 X-ray Source Model. Afterwards with using the equation 1.3. the binding energies have been calculated.

2.2.5. Scanning electron microscopy (SEM) analyse

The samples morphologies have been characterized by utilizing the Thermo Scientific Quattro S scanning electron microscope (SEM).

3. RESULTS AND DISCUSSION

The PEC performance of the samples were evaluated with the OCP, LSV and Impedance spectroscopy measurements. These methods were chosen in order to give an insight and determine the photoelectrochemical properties of the photoanodes. Also to show the possible effects of the surface modification such as light absorption properties, the UV-Vis analysis were conducted on the bare and titanium modified hematite samples. To confirm the formation of the titanium dioxide overlayer on the hematite surface, XPS analysis was performed, and the morphologies were examined with the SEM micrographs and discussed in this section.

3.1. Effect of the Surface Modification

In this study, the effects of the surface modification have been evaluated. With different concentrations of TALH solution (0.5, 2.5, and 5 mmol L⁻¹), prepared hematite samples have been immersed in the solutions, afterwards the samples were cleaned with pure water and dried. Following the immersion step, samples were heat treated (calcination) in air and argon atmospheres at various temperatures and times for the surface modification [3].

3.1.1. Photoelectrochemical tests

Under a standard solar irradiation, the PEC tests were conducted in a NaOH electrolyte solution with 0.1 M with the utilization of a potentiostat. Each samples were illuminated with a solar simulator light source that produces an intensity of 1000 W/cm² illumination. Using OCV, LSV and EIS analysis, we have observed the effect of the surface modification applied with different concentrations of TALH solutions and the various calcination atmospheres (air and argon) and temperatures [2].

Open-circuit voltage (OCV) analysis

The OCP measurements have been evaluated here in this section of the bare and surface modified hematite samples (0,5 / 2,5 / 5 mmolL⁻¹) respectively. Here we observed that the voltage went to the negative side from positive which indicates that these samples were n-type semiconductors. When an electron moves from valence to the conduction band, its fermi energy level increases and approaches more cathodic potentials. Potential deviations between the dark and light conditions of the surface-modified and bare hematite photoanodes have been observed in these experiments [1]. According to these results, we have observed that the surface

modification process has slightly increased the potential deviation between the dark and illuminated conditions of the photoanode, though this deviation increase rather stayed in a low level.

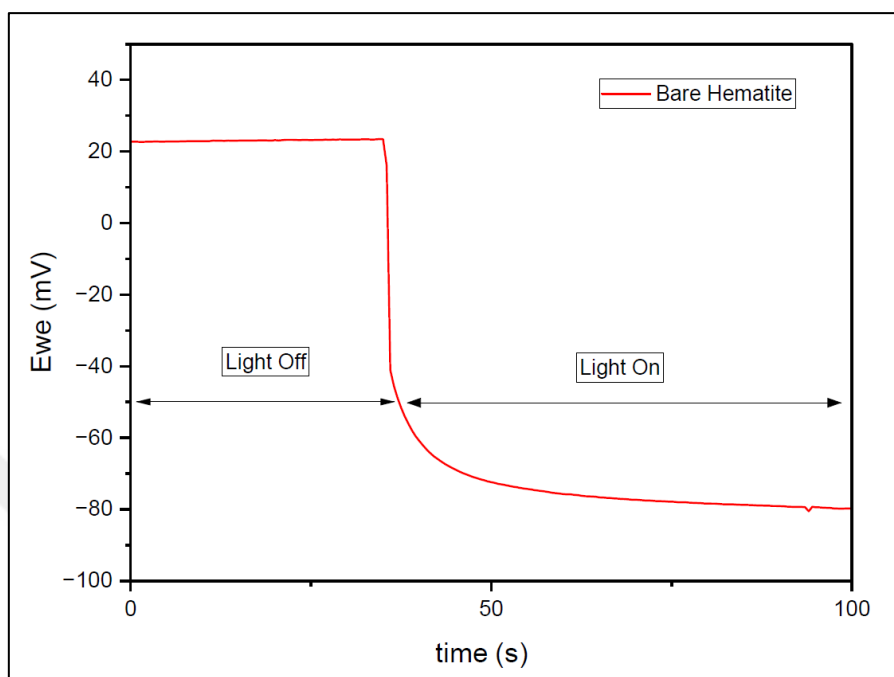


Figure 3. 1. Open circuit potential analysis of bare hematite produced in the air atmosphere at 550 °C for 30 minutes.

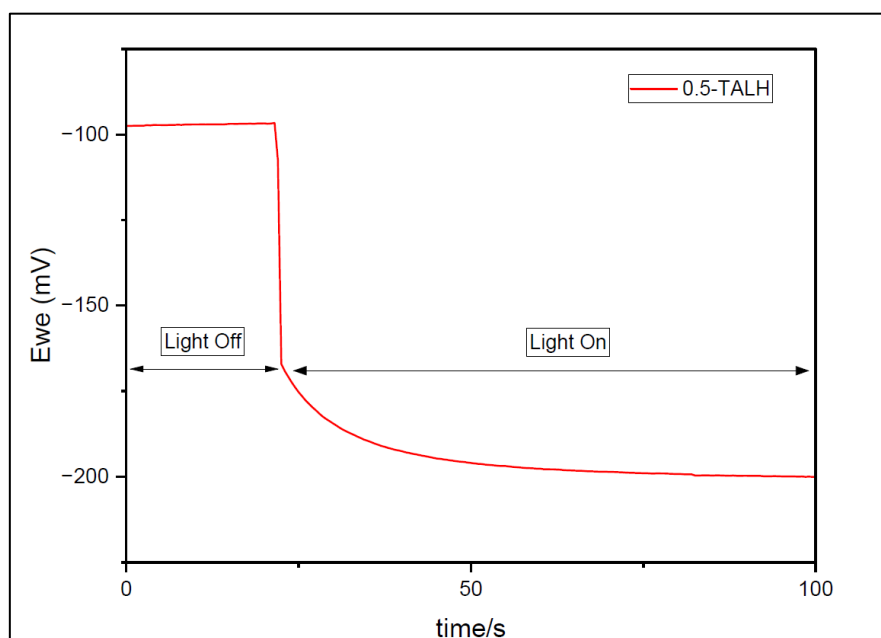


Figure 3. 2. Open circuit potential analysis of surface modified hematite, immersed in 0.5 mmol/L TALH solution for 1 hour and calcinated in air atmosphere at 350 °C for 1 hour.

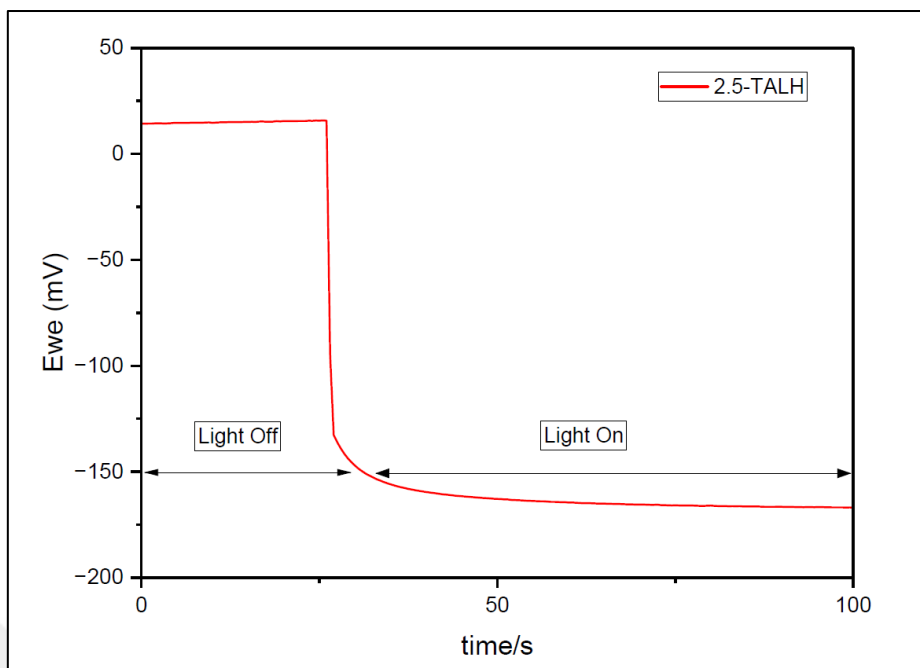


Figure 3. 4. Open circuit potential analysis of surface modified hematite, immersed in 2.5 mmol/L TALH solution for 1 hour and calcinated in air atmosphere at 350 °C for 1 hour.

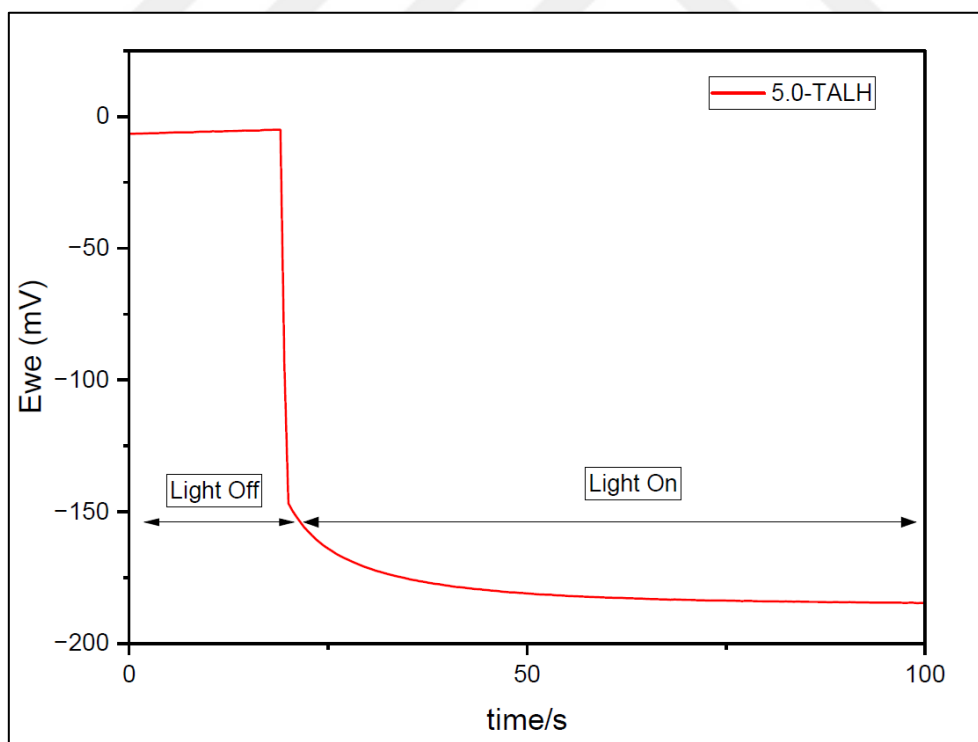


Figure 3. 3. Open circuit potential analysis of surface modified hematite, immersed in 5.0 mmol/L TALH solution for 1 hour and calcinated in air atmosphere at 350 °C for 1 hour.

The surface modified hematite with the use of 2.5 TALH concentrated solution exhibited approximately 170 mV potential drop while the bare hematite exhibited approximately 100 mV. The improved potential drop suggests an improvement in photogenerated charge separation and transport compared to the bare hematite. The TiO₂ overlayer here most likely enhanced the surface charge dynamics and reduced the recombination losses. This behavior positively effects the PEC efficiency by increasing the photocurrent and the photoelectrochemical performance [1-3].

Linear sweep voltammetric (LSV) analysis

The previous studies showed that the lower oxygen content thermal oxidation environment has been enhanced the photocurrent densities of the hematite photoanodes. The highest photocurrent density was observed when the thermal oxidation conducted in the argon atmosphere [2].

In this section in order to show the effect of the surface modification, first the hematite samples produced in air atmosphere and were calcinated in air atmosphere were evaluated. After that to observe the effect of calcination atmosphere, the samples calcinated in argon atmosphere have been evaluated.

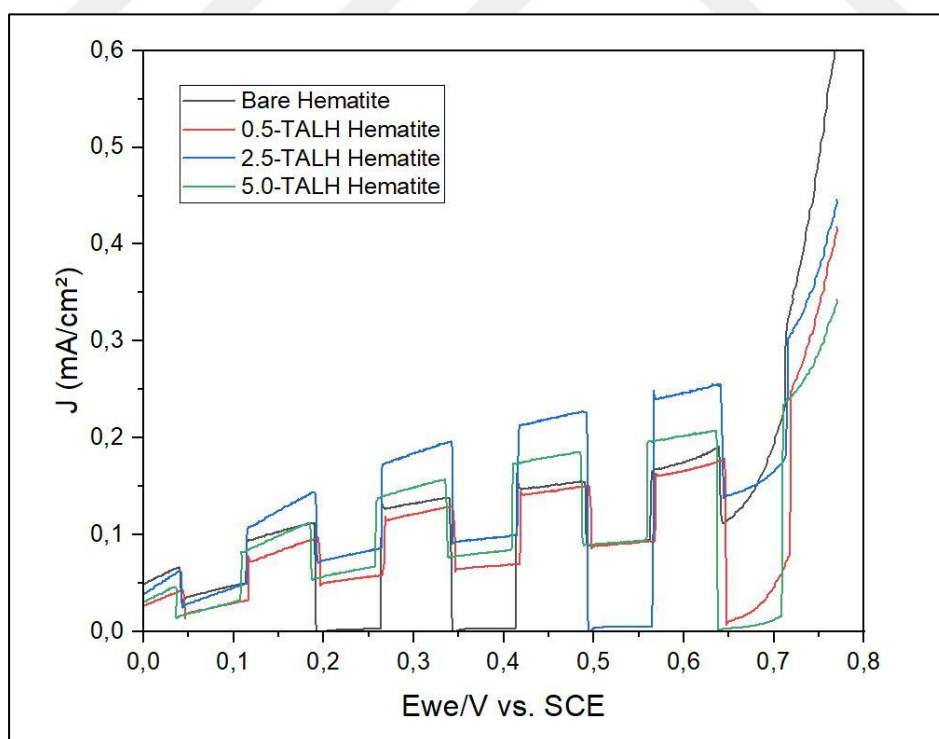


Figure 3. 5. LSV analysis under dark and illuminated conditions. Bare hematite produced in air atmosphere, surface modified hematite samples were immersed in TALH solutions for 1 hour and calcinated in air atmosphere at 350°C for 1 hour.

In the figure 3.5. the photocurrent densities monitored at 0,6 V versus the SCE, the hematite (α - Fe_2O_3) sample modified with 2,5 mmol/L TALH solution has showed the maximum value of 0,24 mA/cm², while the bare hematite has showed 0,16 mA/cm² as the minimum value. In order to observe the effect of the immersion time on the surface modification, various TALH concentrations with differant immersion times have been evaluated.

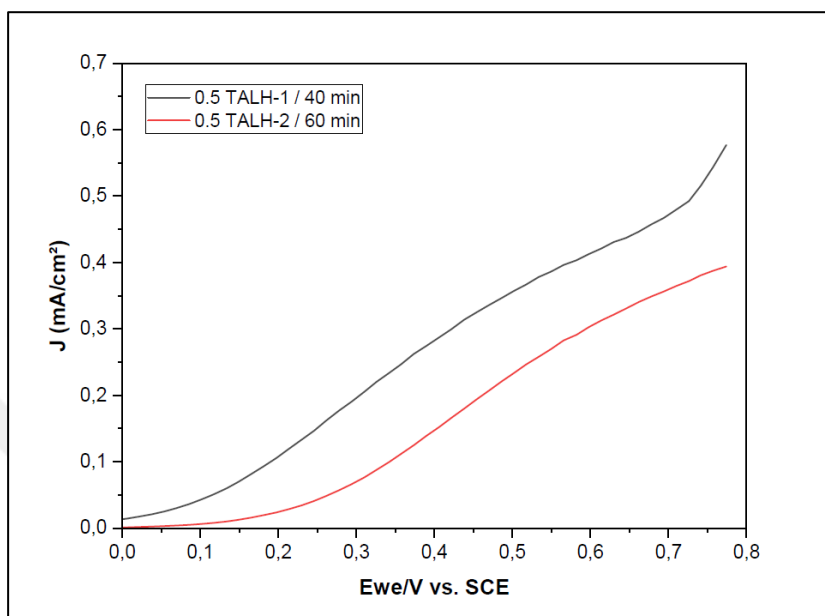


Figure 3. 6. LSV analysis of modified hematite samples. Immersed in 0.5 mmol/L TALH solution with various immersion times (40-60 min), afterwards calcinated in argon atmopshere at 350°C for 1 hour.

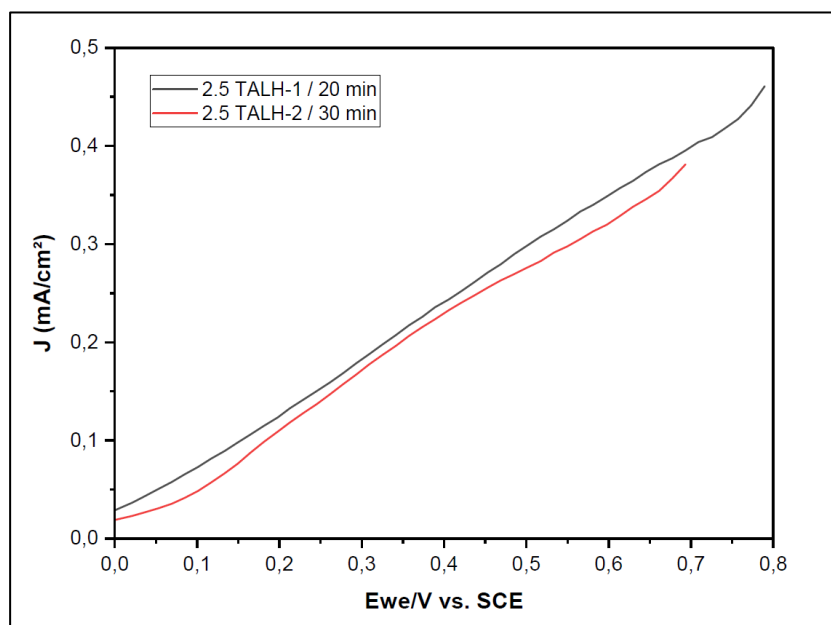


Figure 3. 7. LSV analysis of modified hematite samples. Immersed in 2.5 mmol/L TALH solution with various immersion times (20-30 min), afterwards calcinated in argon atmopshere at 350°C for 1 hour.

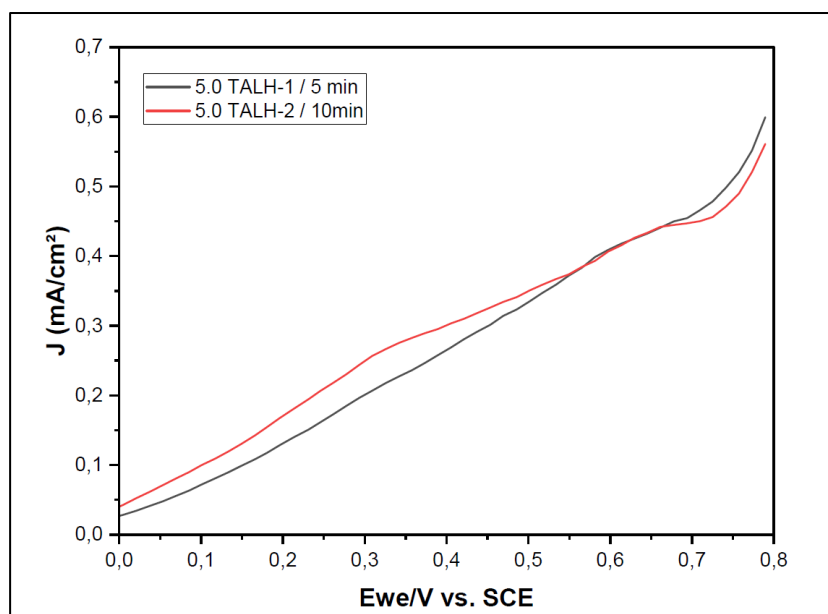


Figure 3. 8. LSV analysis of modified hematite samples. Immersed in 5.0 mmol/L TALH solution with various immersion times (5-10 min), afterwards calcinated in argon atmosphere at 350°C for 1 hour.

Results in this sections reveals that the immersion time in the surface modification process slightly effected the photo current densities of the photoanodes. With lower concentrations this effect has more clearly observed like shown in the figure 3.6. The highest photocurrent density observed here at 0,6 V versus the SCE was 0.42 mA/cm² for the modified hematite with 0.5 mmol/L TALH solution for 10 minutes as shown in figure 3.8.

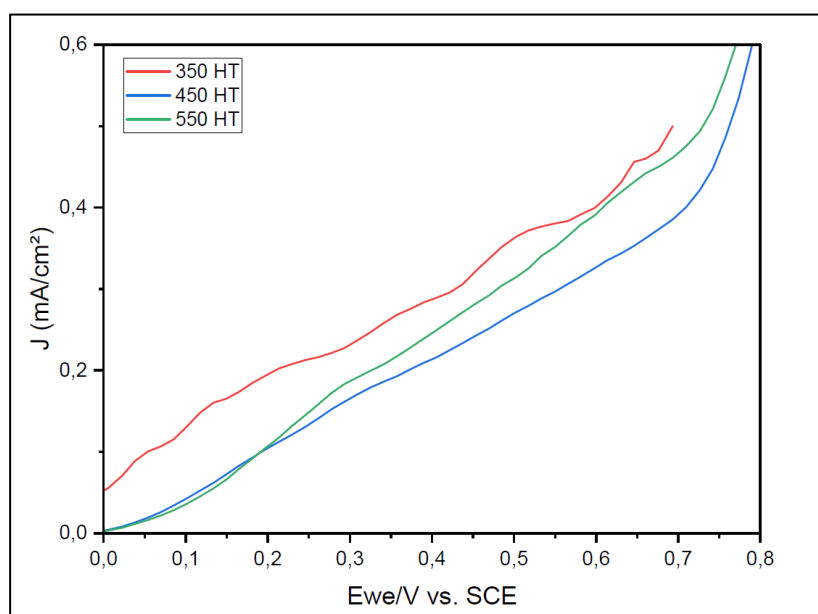


Figure 3. 9. LSV analysis of surface modified samples with various calcination temperatures. Immersed in 2.5 mmol/L TALH solution for 1 hour, calcinated at various temperatures (350-450-550 °C) in argon atmosphere for 1 hour.

For the investigation of the effect of calcination temperature, the samples modified with 2.5 mmol/L TALH solution have been calcinated for 1 hour with various calcination temperatures (350,450 and 550 °C) in argon atmosphere as shown in figure 3.9. It was observed that the calcination temperature also effected the photocurrent density. The photocurrent densities are here monitored at 0,6 V versus the SCE, the 350 HT sample has showed the highest value as 0.41 mA/cm². The results indicated that the calcination process conducted in argon atmosphere has slightly enhanced the photocurrent density of the photoanode. The ideal calcination temperature was determined as 350°C. Lower temperatures probably prevented the excessive grain growth and maintain active surface sites for charge transfer. The LSV data highlights that lower calcination temperatures (350°C) favor improved PEC performance. The performance degradation observed at higher temperatures (450°C and 550°C) is also consistent with the literature reports indicating the trade-off between crystallinity, surface states, and active sites during thermal treatments [3-26].

Electrochemical impedance analysis

The electrochemical impedance spectroscopy measurements have been conducted to show the charge transfer kinetics of the photoanode. The following measurements are conducted with the equivalent circuit model shown in figure 3.10.

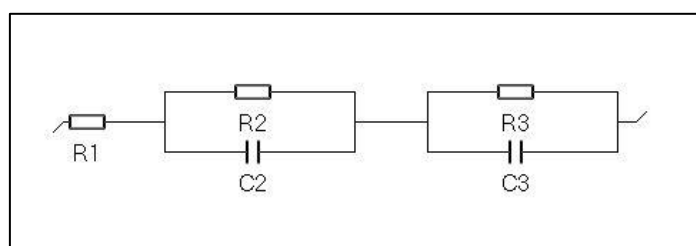


Figure 3. 10. Equivalent circuit model illustration that used in the impedance analysis.

The provided circuit model includes R_1 which refers as the solution resistance, R_2 and R_3 refers the resistances corresponding to interfacial charge transfer and C_2 and C_3 capacitances representing charge storages at the interfaces.

For this experiment to show the effect of the surface modification only bare and titanium modified hematite samples have been used. The bare hematite sample was produced in an argon atmosphere in the conditions shown in table 2.1. For the titanium-modified sample, the surface

modification involved immersing the hematite in a 2.5 mmol/L TALH solution for 1 hour, followed by a calcination process in an argon atmosphere at 350°C for 1 hour.

In the figure 3.11. the nyquist plots(z-fitted) have b Re(Z), Ohms represents the real part of impedance which is associated with resistive elements in the electrochemical system such as charge transfer resistance and solution resistance. The $-Im(Z)$ on the y-axis shows the imaginary part of the impedance, which is linked to capacitive or inductive responses such as charge storage at interfaces [3-18].

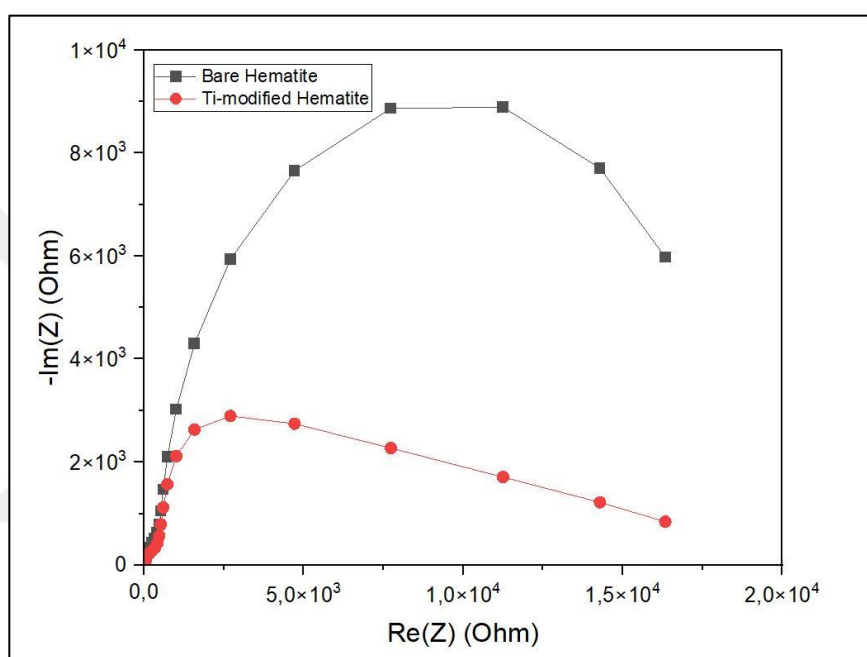


Figure 3. 11. Nyquist plots (z-fitted) of the bare and titanium modified hematite samples under illuminated conditions. Bare hematite produced in argon atmosphere, Ti-modified hematite sample immersed in 2.5 mmol/L TALH solution for 1 hour and calcinated in argon atmosphere at 350 °C for 1 hour.

Table 3. 1. Fitting results for EIS analysis of the samples.

| Samples | R_s (Ω) | C_{sc} (F) | R_{sc} (Ω) | C_h (F) | R_{ct} (Ω) |
|-----------------------------|--------------------|--------------|-----------------------|-----------|-----------------------|
| Bare Hematite | 36,54 | 15,346 | 467,9 | 33,23 | 18090 |
| Ti modified Hematite | 51,98 | 40,998 | 5790 | 19,04 | 249,8 |

Here in this experiment the bare hematite photoanode showed a larger semicircle and indicated a higher impedance, this refers to the poor charge transfer kinetics at the hematite/electrolyte interface. The titanium modified hematite showed a smaller semicircle which shows that the interfacial charge transfer process have been improved with the surface modification process.

As the result the surface modification with titanium dioxide have been increased the charge transfer characteristics of hematite and improved PEC efficiency. According to the impedance analysis this improvement attributed to reduced charge transfer resistance and better interfacial properties resulting as a more efficient photoanode fabricated with the surface modification [3].

3.1.2. UV-Vis analysis

The bare hematite and titanium modified hematite samples were evaluated with UV-Vis spectroscopy in order to measure the absorbance of light in the ultraviolet and visible regions of the spectrum (200-800 nm) and presented in figure 3.12. below.

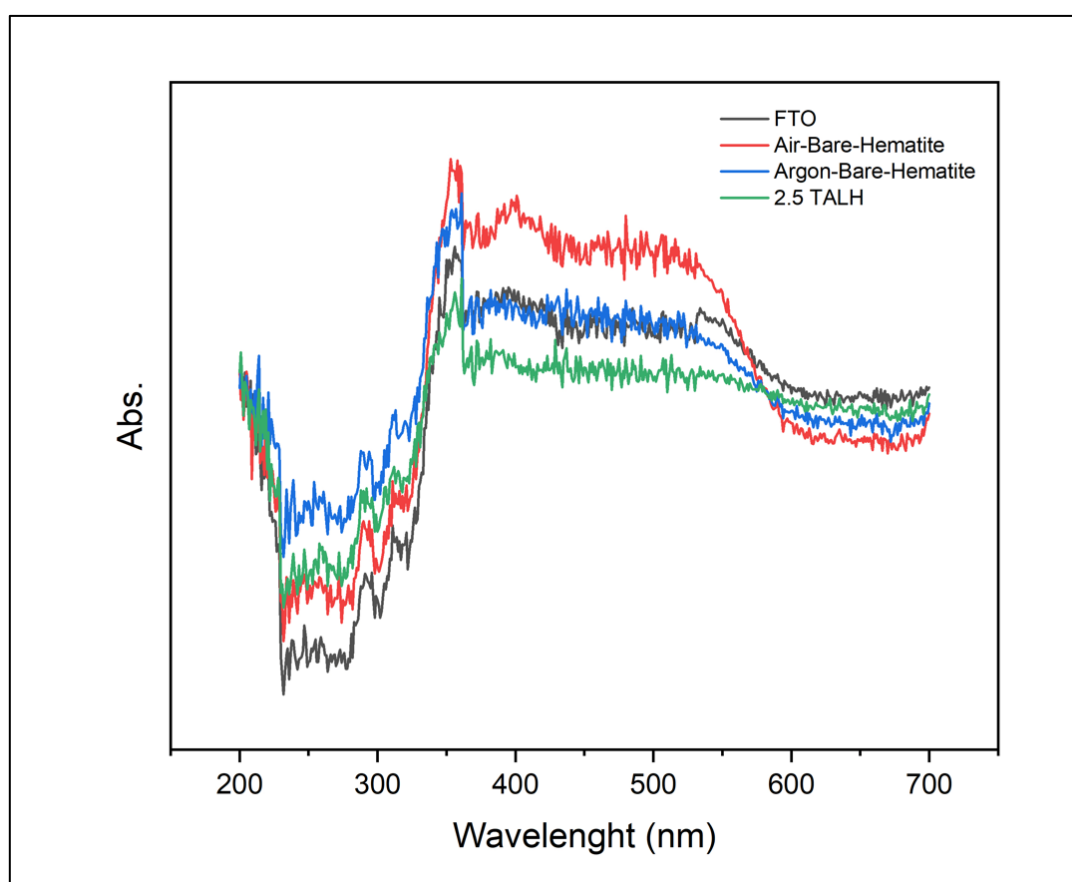


Figure 3. 12. Shows the UV-Vis absorption spectra of the samples. Bare hematite produced in air and argon atmosphere, titanium modified hematite immersed in 2.5 mmol/L TALH solution for 1 hour and calcinated in argon atmosphere at 350 °C for 1 hour.

For this analysis the bare hematite sample showed the highest visible light absorption, while the titanium modified hematite sample showed the lowest light absorption. The higher light absorption may result in a better PEC performance if the factors such as electron-hole recombination is controlled. Despite the surface modification technique have been decreased the

light absorption of the hematite, still the PEC test results showed the higher photo-current densities on titanium modified hematite sample. It is possible that the titanium dioxide modification enhanced the properties such as charge transfer and compensate the poor light absorption and reveal a slightly efficient photoanode. [3-18].

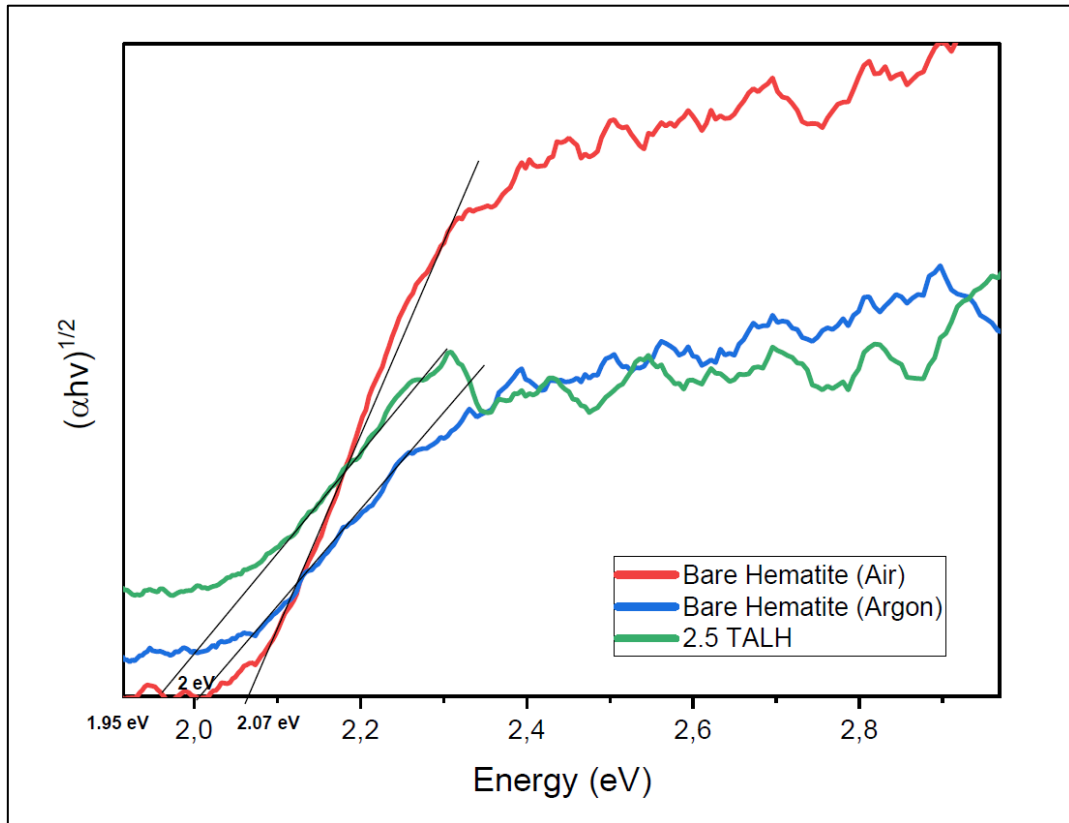


Figure 3. 13. Shows the Tauc Plots of bare and titanium modified hematite samples.

From the absorption data, with using the tauc equation (1.2) the band gaps of the materials have been calculated and presented in figure 3.13. with the Tauc Plots. The titanium modified hematite samples bandgap calculated 1.95 eV while the bare hematite fabricated in air atmosphere was calculated 2.07 eV and the bare hematite fabricated in argon atmosphere calculated 2.0 eV respectively. The possible reasons for the slight bandgap decrease observed in the titanium modified sample could be the arising Mid-Gap states which introduce defect states and narrowing the bandgap. Some other reason could be the charge transfer interaction between titanium modified surface and hematite interface, this phenomena can result with the reduction of energy difference between the valance and conduction bands of the semiconductor [2-3-18].

3.1.3. X-ray photospectrometry (XPS) analysis

The XPS analysis were carried out to provide data from the surface modification of the hematite. The figure 3.14. presents the XPS analysis focused on the binding energy range of

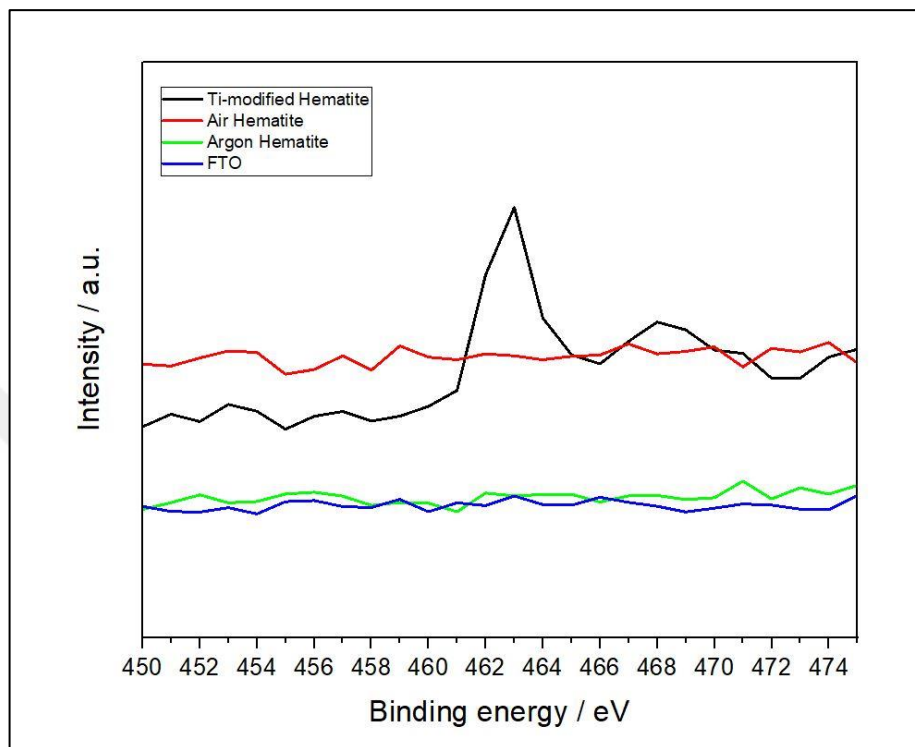


Figure 3. 14. XPS analysis of the bare and titanium modified hematite samples focused in the binding energy range of 450-474 eV. Ti-modified hematite sample immersed in 2.5 mmol/L TALH solution for 1 hour and calcinated in argon atmosphere at 350 °C for 1 hour.

450-475 eV. This range was selected here in order to show the specific titanium peaks such as Ti 2p more effectively. Here in the figure 3.14. the titanium modified hematite clear peak have been observed at 462-464 eV range, which corresponds with the Ti 2p core level range. The presence of this titanium peak that have been only observed on the surface modified hematite sample confirms the presence of titanium dioxide overlayer have been achieved on the surface of the hematite with the surface modification technique. Titanium dioxide overlayer observed through the XPS analysis here acts as a passivation layer, reducing the surface defect states and recombination centers. The total PEC efficiency of the titanium-modified hematite sample have been slightly increased as a result of fewer surface imperfections and recombination centers. This results also alligns with the findings from Impedance analysis, where a reduced charge transfer resistance was observed for the titanium modified hematite sample [3-24].

3.1.4. SEM (Scanning electron microscopy) analysis

Investigation of the surface morphology have been carried out with the bare and titanium modified hematite ($\alpha\text{-Fe}_2\text{O}_3$) samples, both thermal oxidation and calcination processes conducted in argon atmosphere. The surface modification of the titanium modified hematite sample have been conducted with 2.5 mmol/L TALH solution.

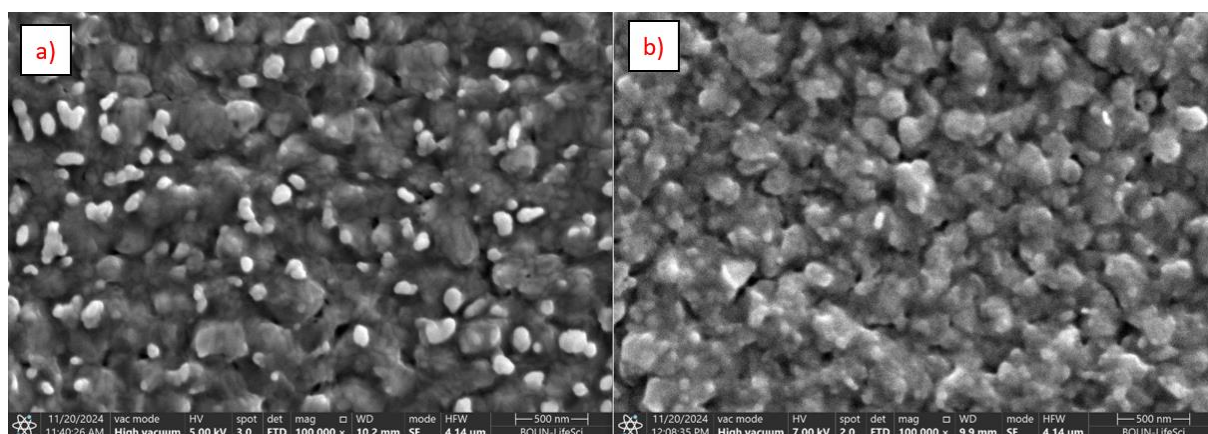


Figure 3. 15. SEM micrographs of the a) bare hematite produced in argon atmosphere b) titanium modified hematite, immersed in 2.5 mmol/L TALH for 1 hour, calcinated in argon atmosphere at 350 °C for 1 hour.

The morphology observed with the SEM analysis, Figure 3.15. shows the SEM images of the samples observed with Everhart-Thorley detector in the secondary electron mode. It was observed that after applying the surface modification process, the titanium modified hematite samples revealed a more homogeneous particle distribution. The reduced visibility of individual grain boundaries suggests the formation of a thin and conformal titanium dioxide film on the surface area. According to the PEC tests, this surface modification lead to a reduction of the surface recombination sites and slightly improved charge separation of the sample in photocataytic applications [3-25].

4. CONCLUSION

Hematite samples were successfully fabricated by the thermal oxidation of iron (Fe) thin films. Surface modification of the hematite samples were carried out using a straightforward method involving a titanium-based water-soluble complex, specifically titanium bis(ammonium lactate) dihydroxide (TALH). The modification process involved immersing the hematite in the TALH solution, followed by a gentle heat treatment (calcination), which resulted in the formation of a titanium dioxide (TiO_2) overlayer on the surface of the hematite. The optimal surface modification was achieved with using the 5.0 mmol/L TALH concentration, with a 10-minute immersion time followed with 1-hour of calcination step in an argon atmosphere. This treatment yielded the most enhanced photoelectrochemical (PEC) performance among all tested samples. Specifically, the titanium-modified hematite, with both thermal oxidation and calcination conducted in an argon atmosphere, exhibited a photocurrent density of 0.42 mA/cm^2 at 0.6 V versus SCE, representing the highest efficiency recorded in this study.

In conclusion, the surface modification of hematite photoanodes with a TiO_2 layer has demonstrated a modest enhancement in PEC performance. Calcination step conducted in argon atmosphere showed an increase on the PEC performance. This improvement is attributed to increased charge transfer efficiency, reduced recombination losses, decreased charge transfer resistance, and minor modifications to the light absorption properties of the hematite photoanodes. The findings of this study showed that with using this surface modification method TiO_2 coating on hematite surface can successfully be achieved and has minor beneficial effects on the PEC hydrogen production efficiency of the hematite.

REFERENCES

- [1] Sivula, K., le Formal, F., & Grätzel, M. (2011). Solar Water Splitting: Progress Using Hematite (α -Fe₂O₃) Photoelectrodes. *ChemSusChem*, 4(4), 432–449. <https://doi.org/10.1002/CSSC.201000416>
- [2] Güler, Fatma Betül Yılmaz. “The Effect of Oxidation Atmosphere on Morphology and Hydrogen Production Efficiency of Hematite Photo Anode Produced by Oxidation of Deposited Fe Film”, Marmara Üniversitesi (Turkey)
- [3] Ahmed, M. G., Kretschmer, I. E., Kandiel, T. A., Ahmed, A. Y., Rashwan, F. A., & Bahnemann, D. W. (2015). A facile surface passivation of hematite photoanodes with TiO₂ overlayers for efficient solar water splitting. *ACS applied materials & interfaces*, 7(43), 24053–24062. <https://doi.org/10.1021/acsami.5b07065>.
- [4] Niaz, S., Manzoor, T., & Pandith, A. H. (2015). Hydrogen storage: Materials, methods and perspectives. *Renewable and Sustainable Energy Reviews*, 50, 457–469. <https://doi.org/10.1016/j.rser.2015.05.011>.
- [5] Walter, M. G., Warren, E. L., McKone, J. R., Boettcher, S. W., Mi, Q., Santori, E. A., & Lewis, N. S. (2010). Solar water splitting cells. *Chemical reviews*, 110(11), 6446–6473. <https://doi.org/10.1021/cr1002326>.
- [6] Lin, Y., Yuan, G., Sheehan, S., Zhou, S., & Wang, D. (2011). Hematite-based solar water splitting: challenges and opportunities. *Energy & Environmental Science*, 4(12), 4862–4869. <https://doi.org/10.1039/C1EE01850G>.
- [7] Jha, B. K., Chaule, S., & Jang, J. H. (2024). Enhancing photocatalytic efficiency with hematite photoanodes: principles, properties, and strategies for surface, bulk, and interface charge transfer improvement. *Materials Chemistry Frontiers*, 8(10), 2197–2226. DOI: 10.1039/D3QM01100C.
- [8] Meng, Q., Wang, Z., Chai, X., Weng, Z., Ding, R., & Dong, L. (2016). Fabrication of hematite (α -Fe₂O₃) nanoparticles using electrochemical deposition. *Applied Surface Science*, 368, 303–308. <https://doi.org/10.1016/j.apsusc.2016.02.007>.
- [9] Liu, R.; Zheng, Z.; Spurgeon, J.; Yang, X. Enhanced Photoelectrochemical Water-Splitting Performance of Semiconductors by Surface Passivation Layers. *Energy Environ. Sci.* 2014, 7, 2504–2517. <https://doi.org/10.1039/C4EE00450G>.
- [10] Hu, S.; Shaner, M. R.; Beardslee, J. A.; Lichterman, M.; Brunschwig, B. S.; Lewis, N. S. Amorphous TiO₂ Coatings Stabilize Si, GaAs, and GaP Photoanodes for Efficient Water Oxidation. *Science* 2014, 344, 1005–1009. <https://doi.org/10.1126/science.1251428>.
- [11] Ahmed, A. Y.; Oekermann, T.; Lindner, P.; Bahnemann, D. Comparison of the Photoelectrochemical Oxidation of Methanol on Rutile TiO₂ (001) and (100) Single Crystal Faces Studied by Intensity Modulated Photocurrent Spectroscopy. *Phys. Chem. Chem. Phys.* 2012, 14, 2774–2783. <https://doi.org/10.1039/C2CP23416E>.
- [12] Klahr, B.; Gimenez, S.; Fabregat-Santiago, F.; Hamann, T.; Bisquert, J. Water Oxidation at Hematite Photoelectrodes: The Role of Surface States. *J. Am. Chem. Soc.* 2012, 134, 4294–4302. <https://doi.org/10.1021/ja210755h>.
- [13] F. Feng, et al., Boosting hematite photoelectrochemical water splitting by decoration of TiO₂ at the grain boundaries, *Chem. Eng. J.*, 2019, 368, 959–967. <https://doi.org/10.1016/j.cej.2019.03.005>.
- [14] Li, F., Jian, J., Wang, S., Zhang, Z., Jia, L., Guan, X., ... & Wang, H. (2023). TiO₂ passivation layers with laser derived pn heterojunctions enable boosted photoelectrochemical performance of α -Fe₂O₃ photoanodes. *Chemical Engineering Journal*, 461, 141872. <https://doi.org/10.1016/j.cej.2023.141872>.

- [15] Rustad, J. R.; Wasserman, E.; Felmy, A. R. Molecular Modeling of the Surface Charging of Hematite: II. Optimal Proton Distribution and Simulation of Surface Charge versus pH Relationships. *Surf. Sci.* 1999, 424, 28-35. [https://doi.org/10.1016/S0039-6028\(99\)00009-6](https://doi.org/10.1016/S0039-6028(99)00009-6).
- [16] Smart, T. J., Chen, M., Grieder, A. C., Urena Baltazar, V., Bridges, F., Li, Y., & Ping, Y. (2021). The critical role of synthesis conditions on small polaron carrier concentrations in hematite—A first-principles study. *Journal of Applied Physics*, 130(24). <https://doi.org/10.1063/5.0074698>.
- [17] Ager, J. W., Shaner, M. R., Walczak, K. A., Sharp, I. D., & Ardo, S. (2015). Experimental demonstrations of spontaneous, solar-driven photoelectrochemical water splitting. *Energy & Environmental Science*, 8(10), 2811-2824. <https://doi.org/10.1039/C5EE00457H>
- [18] Chen, Z., Dinh, H. N., & Miller, E. (2013). Photoelectrochemical water splitting: standards, experimental methods, and protocols. <https://doi.org/10.1007/978-1-4614-8298-7>.
- [19] Wang, L., Nguyen, N. T., & Schmuki, P. (2016). A facile surface passivation of hematite photoanodes with iron titanate cocatalyst for enhanced water splitting. *ChemSusChem*, 9(16), 2048-2053. <https://doi.org/10.1002/cssc.201600462>.
- [20] Mullet, M., Fievet, P., Szymczyk, A., Foissy, A., Reggiani, J. C., & Pagetti, J. (1999). A simple and accurate determination of the point of zero charge of ceramic membranes. *Desalination*, 121(1), 41-48. [https://doi.org/10.1016/S0011-9164\(99\)00006-5](https://doi.org/10.1016/S0011-9164(99)00006-5)
- [21] Dawood, F., Anda, M., & Shafiullah, G. M. (2020). Hydrogen production for energy: An overview. *International Journal of Hydrogen Energy*, 45(7), 3847-3869.
- [22] Förster, H. (2004). *UV/VIS Spectroscopy* (Vol. 4). Springer, Berlin, Heidelberg. <https://doi.org/10.1007/B94239>.
- [23] Zhu, L., Lu, Q., Lv, L., Wang, Y., Hu, Y., Deng, Z., ... & Teng, F. (2017). Ligand-free rutile and anatase TiO₂ nanocrystals as electron extraction layers for high performance inverted polymer solar cells. *RSC advances*, 7(33), 20084-20092. <https://doi.org/10.1039/C7RA00134G>
- [24] Krishna, D. N. G., & Philip, J. (2022). Review on surface-characterization applications of X-ray photoelectron spectroscopy (XPS): Recent developments and challenges. *Applied Surface Science Advances*, 12, 100332. <https://doi.org/10.1016/j.apsadv.2022.100332>
- [25] Popescu, G. et al. (2020). "Morphological and Structural Analysis of Hematite Thin Films by SEM." *Journal of Material Science Research*, 8(4), 123-130. DOI:10.1016/j.optmat.2020.110496.
- [26] Phuan, Y. W., Chong, M. N., Zhu, T., Yong, S. T., & Chan, E. S. (2015). Effects of annealing temperature on the physicochemical, optical and photoelectrochemical properties of nanostructured hematite thin films prepared via electrodeposition method. *Materials Research Bulletin*, 69, 71-77. <https://doi.org/10.1016/j.materresbull.2014.12.059>